ACS APPLIED MATERIALS & INTERFACES

www.acsami.org

Research Article

Light-driven Locomotion of Underwater Bubbles on Ultrarobust Paraffin-impregnated Laser-ablated Fe_3O_4-doped Slippery Surfaces

Zhouchen Huang,[a] Chao Chen,[a] Xinghao Wang, Rui Li, Yucheng Bian, Suwan Zhu, Yanlei Hu, Jiawen Li,* Dong Wu,* and Jiaru Chu

Cite This: *ACS Appl. Mater. Interfaces* 2021, 13, 9272–9280

Read Online

ACCESS | Metrics & More | Article Recommendations | Supporting Information

ABSTRACT: Manipulating underwater bubbles (UGBs) is realized on morphology-tailored or stimuli-responsive slippery lubricant-impregnated porous surface (SLIPS). Unfortunately, the volatile lubricants (*e. g.*, silicone oil, ferrofluid) greatly decrease their using longevity. Designed is light-responsive paraffin-infused Fe_3O_4-doped slippery surface (LR-PISS) by incorporation of hybrid lubricants and superhydrophobic micropillar-arrayed elastometric membranes resulted from one-step femtosecond laser vertically scanning. Upon LR-PISS, the dynamic motion control bwteen pinning and sliding along free routes over UGB could be realized by alternately loading/discharging NIR-trigger. The underlying principle is that when the NIR was applied, UGB would be actuated to slide along the NIR trace because the irradiated domain melts for a slippery surface within 1.0 s. Once the NIR is removed, the liquefied paraffin would be reconfigured to solid phase for pinning a moving UGB within 0.5 s. Newly explored hydrokinetics imparts us with capability of steering UGBs to arrange any desirable patterns and switch light-path behaving as the light-control-light optical shutter. In comparison with previously reported SLIPS, current LR-PISS unfolds unparalleled ultrarobust antidisturbance ability even in flowing liquid ambient. More significantly, even subjected to physical damage, underwater LR-PISS is capable of in situ self-healing within 13 s under the assistance of remote NIR. The results here could inspire the design of robust bubble manipulator and further boost their applications in optofluidics and all-optical modulators.

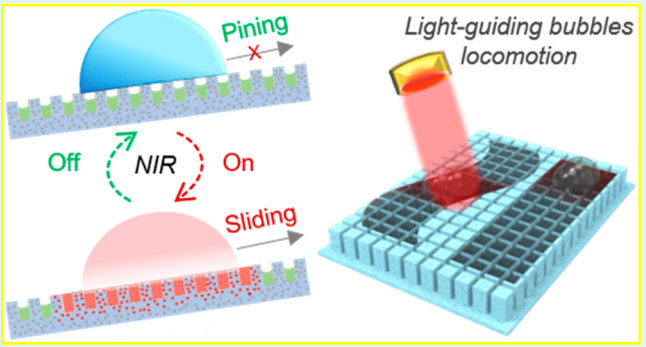

KEYWORDS: *light-responsive slippery surface, underwater bubbles manipulation, switchable wettability, ultrarobust stability, in situ self-healing*

1. INTRODUCTION

Manipulating the underwater gas bubble (UGB) behavior in liquid environment is of great importance because of its potential applications in a wide variety of fields over both academic research and industrial production, such as bubble transport in microfluidics,[1] wastewater treatment,[2] electrochemistry with bubble participation,[3,4] repair of transport pipeline,[5−8] and so on. In recent years, some reported approaches over bubble manipulation upon two typical interfaces featured as superhydrophobic surface and slippery liquid impregnated porous surface (SLIPS). For clarification, the first classification listed here, that is, the most of gas bubble manipulation strategies are controlled via shaped superhydrophobic nonslippery surfaces, which enables UGB to move directly by a driving force arising from the asymmetric morphology. For instance, Yu et al. developed a superhydrophobic copper cone by electro-etching and a subsequent hydrophobized treatment overnight, which is responsible for spontaneously and directionally actuating UGB toward arbitrary directions by a classical driving force, that is, Laplace pressure difference derived from the conical morphology.[9] Following this method, Zhu et al. designed an asymmetric superhydrophobic dual-orbit on a hybrid stainless/PDMS by femtosecond laser ablation, which was also competent for achieving the spontaneous movement of UGBs on the basis of Laplace pressure difference.[10] More recently, Jiang and his coworkers reported a Janus triangular electrode with dual directionality featured as having an axial asymmetric morphology and a longitudinal wettability gradient (a top superhydrophobic surface and a bottom hydrophobic one). This newly explored surface imparts in situ highly effective separations, transportation and collection over H_2/O_2.[11] Unfortunately, in terms of UGBs steering, all of these

Received: December 23, 2020
Accepted: February 2, 2021
Published: February 9, 2021

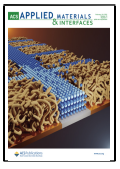

https://dx.doi.org/10.1021/acsami.0c22717
ACS Appl. Mater. Interfaces 2021, 13, 9272–9280

Table 1. Comparisons of Key Parameters for Stimuli-Responsive SLIPS

materials	method	response	dynamicmotion control	stability	self-heal in water	ref.
hydrophobic silica nanoparticle/PDMS modified filter paper	chemical modification	no	can not	volatile	can not	14
iron powder/PDMS/silicone oil	N/A	magnetic	yes	volatile	can not	15
Fe_3O_4- NPs/PDMS platform/Silicone oil	one-step femtosecond laser ablation	light	yes	volatile	can not	16
Ni−Ti alloy sheet/ferrofluid	one-step femtosecond laser ablation	magnetic	yes	volatile	can not	17
Fe_3O_4-NPs/PDMS platform/paraffin wax	one-step femtosecond laser ablation	light	yes	ultrarobust	yes (13 s)	this work

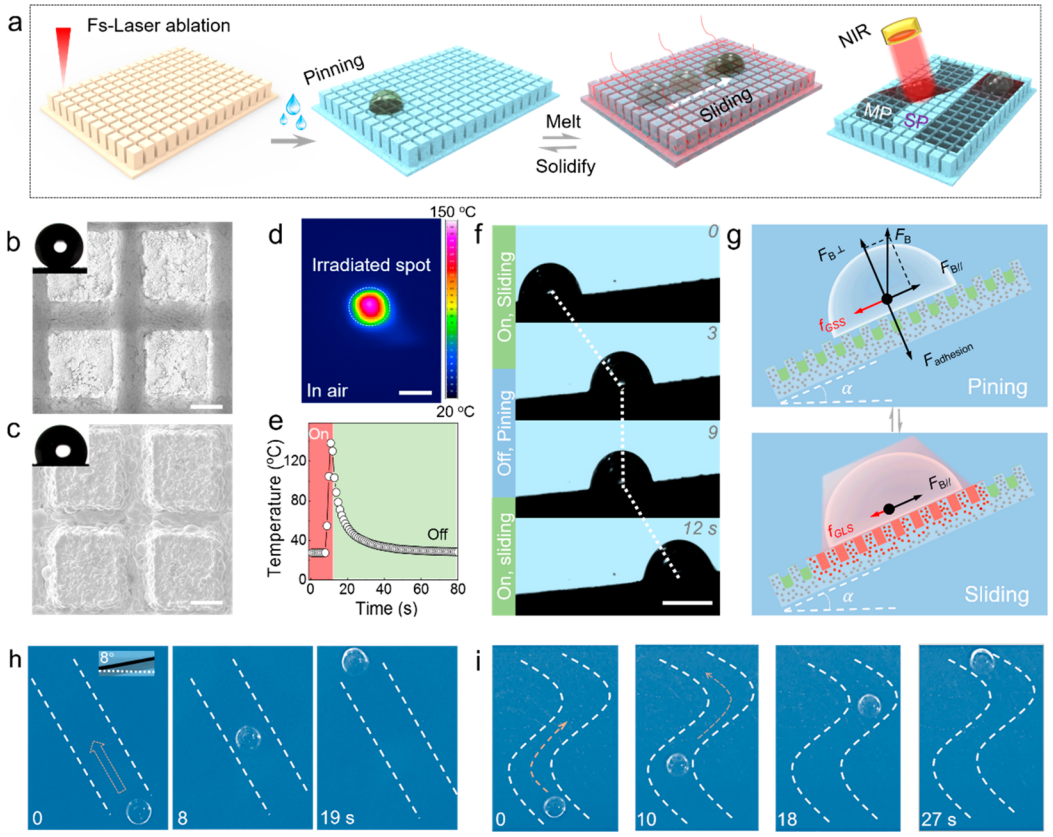

Figure 1. Facile fabrication of smart LR-PISS and its Characterizations. (a) Schematic diagram for illustrating the fabrication strategy composed of superhydrophobic micropillar-arrayed Fe_3O_4-doped PDMS membrane ablated by one-step femtosecond laser and paraffin impregnation. Under the assistance of Fe_3O_4-derived photothermal effect, the steering method over gasous bubble is utilizing a controllable NIR-irradiated trace to introduce desirable slippery routes upon melting the lubricant paraffin wax. SEM clips for superhydrohobic micropillar-arrayed Fe_3O_4/PDMS platform (b) without and (c) with lubricant paraffin wax; The scale bar is 50 μm. The insets represent their corresponding water contact angles (left) and the enlarged SEM imagies (right). (d) Thermal infrared image and (e) temperature variation with irradiated time for NIR-triggered LR-PISS (power density: 1.1 × 10^2 mW cm^{-2}, altitude: 8 cm); The scale bar is 1 cm. (f) Dynamic locomotion control over UGB between sliding and pinning by alternatly loading and discharging NIR-stimuli. (g) Force analysis for a NIR-steering UGB on LR-PISS. The manipulating principle is that the reversibly switch of interface force between larger f_{GSS} and smaller f_{GLS} dominates the pinning and sliding behavior of gasous bubble. Displays of NIR-steering UGBs along (h) sidelong and (i) S-shaped pathways. The results manifest that current LR-PISS is competent for actuating gaseous bubbles toward desirable routes by remotely controlling the NIR-irradiating trace.

superhydrophobic surfaces have pronounced contact angle hysteresis (CAH), together with limited transporting length arising from geometry-dependent feature.[12] Revolutionized surface that overcoming all above-mentioned blockages is highly deserved.

Fortunately, inspired by Nepenthes pitcher plants, Aizenberg and co-workers developed the first paradigm of slippery lubricant-impregnated porous surfaces (SLIPS), which has merits of low CAH, fast self-healed ability after physical damage, in addition to superior repellency in terms of arbitrary simple and complex liquids with suitable lubricants.[13] Accordingly, upon designing isotropic or anisotropic SLIPS, Jiao et al. achived the continuously directional transport and collection over underwater gas/CO_2 bubbles on laser-programmed platforms.[22,23] By taking advantage of lubricant-infused slippery (LIS) surface and shaped asymmetrical structure on hydrophobic silica nanoparticle (HFS) and PDMS modified filter paper, Yu et al. achieved the controlled bubble delivery routes and further the continuous collection and transport of microbubbles.[14] Thereafter, Guo et al.

https://dx.doi.org/10.1021/acsami.0c22717
ACS Appl. Mater. Interfaces 2021, 13, 9272−9280

fabricated a kind of stable magnetic-responsive slippery gel surface by doping iron powder and silicone oil into soft poly(dimethylsiloxane), which was competent for controlling the sliding behaviors of liquids and bubbles by loading/discharging an external magnetic field.[15] To achieve the controllable speed and routes of microbubbles, Chen et. al developed a sort of light-responsive SLIPS based on hydrophobic micropillar-arrayed Fe_3O_4/PDMS films that were ablated by one-step femtosecond (fs) laser, which can work depending on the asymmetric Laplace pressure difference airing from the temperature difference of the lubricants, that is, light-derived wettability gradient force.[16] More recently, for seeking a higher manipulating performance, Zhu et.al designed a magnetism-controlled ferrofluid-infused laser-ablated microstructured surfaces (FLAMS) for accelerating the locomotion of microbubbles above 150 mm/s.[217] In short, all these previously explored ones provide great inspirations for designing functional SLIPS for manipulating UGBs in regard of fabricating techniques and fundamental basis. Nevertheless, three critical blockages arise subsequently: (1) The volatile lubricants (e.g., silicone oil, ferrofluid) greatly shorten the longevity for all above-mentioned SLIPS. (2) Most-reported SLIPSs are not capable of pinning UGB in either static or flowing liquid ambient. (3) To the best of our knowledge,[16,17] the ability to repair SLIPS from damages has been rarely demonstrated (Detailed list can be seen from Table 1). In this regard, the dynamic control of UGB between pinning and sliding on an ultrarobust and self-healed SLIPS, as well as the underlying hydrodynamics, is still a timely challenge and an urgent need.

Herein, we put forward a kind of ultrarobust light-responsive slippery surface (LR-PISS) composed of superhydrophobic micropillar-arrayed Fe_3O_4/polydimethylsiloxane (PDMS) platform enabled by one-step femtosecond laser ablation and lubricant paraffin wax. Thereby, the dynamic locomotion control over UGBs could be reversibly switched between pinning and sliding by loading and discharging the near-infrared (NIR) light with ease. The underlying principle is that when the NIR was applied, the UGBs would be actuated to slide along the NIR trace because the irradiated domain tends to melt for a slippery surface within 1.0 s, which is theoretically favorable for a smaller F_{CAH} under the photothermal effect of Fe_3O_4. Once the near-infrared light is removed, the melted paraffin would be reconfigured to solid phase for pinning a moving UGB within 0.5 s because of the recovered frictional nonslippery one with a larger F_{CAH}. Moreover, we have quantitatively investigated the effect of bubble volume and inclined angles of LR-PISS and lubricant viscosity on the sliding speed of UGBs. The fundamental basis enables us harvesting an optimized value above 5.0 mm/s. Through steering UGBs on LR-PISS, the intentional arrangement, patterning together with programmable light-swtching path could be readily achieved. More importantly, in comparison with previously reported SLIPS, current LR-PISS is more competent for imparting UGBs with ultrastable antidisturbance performance even in flowing liquid environment. Further, this light-triggered SLIPS is capable of in situ self-healing within 13 s after physical damage under the assistance of remote NIR. This work provides profound guidance for researcher to design stable slippery surface for manipulation of gas bubbles in aqueous media.

2. RESULTS AND DISCUSSION

2.1. Facile Fabrication of Smart LR-PISS and Its Characterizations. Figure 1 a shows the fabrication process of light-responsive paraffin-infused Fe_3O_4-doped slippery surface (simplified as LR-PISS) and two typical steps is composed as follows. First, through one-step femtosecond laser cross-scanning, the superhydrophobic pillar-arrayed Fe_3O_4-doped PDMS film (PAF) with a typical water contact angle (WCA) of 155.4 ± 2.3° could be facilely manufactured, where the length (l), width (w), height (h) of a single micropillar and the interval between two adjacent micropillars were measured as 136, 140, 90, and 50 μm, respectively. Therein, fs laser induced superwetting surfaces has merits of long-term wetting stability in comparison with those by traditional chemical hydrophobized methods, which has aroused tremendous attention in most recent years.[24−28] Significantly, XRD patterns that no obvious red/blue shift could be detected in PAF, which revealed that the lattice planes assigned to these materials were not severely damaged or modified by femtosecond laser (Supporting Information (SI) Figure S1). Conducting a further observation by scanning electron microscopy (SEM), the PAF is composed of multiple micropillars, nanoparticles as well as nanopours, which should be conducive for providing a giant capillary force for the infusion and storage of targeted lubricant (Figure 1b and SI Figure S2). In a secondary stage, the thermal spin coating method was employed to uniformly impregnate the molten paraffin into the as-prepared PAF and thus a fresh LR-PISS could be harvested, where the WCA for LR-PISS was measured as 115.2 ± 1.4° and the density of impregnated paraffin wax was estimated as ∼7.25 mg/cm^2 (Figure 1c and SI Figure S3). Therein, by subtracting the characterized height of LR-PISS (with paraffin) from PAF (without paraffin), we could harvest the impregnated thickness of paraffin wax ∼54.5 μm (SI Figure S4). Due to the excellent photothermal conversion efficiency of Fe_3O_4 NPs under the irradiation of NIR, the temperature of irradiated location on LR-PISS is capable of increasing from 25 to 110 °C within 1s in air (Figure 1d,e). In consideration of water having strong absorption over NIR, the whole experiment of temperature variation with irradiated time for NIR-triggered LR-PISS was therefore measured in air. In principle, we could indirectly harvest the temperature variation with irradiated time curve in water by recording the temperature-irradiating time in air, because they all characterize the temperature of air−oil-solid platform (AOS) interface in both air and water surroundings (SI Figure S5). Additionally, the heating radius evolution with irradiated time in water was conducted as shown in SI Figure S6, where we found that the heating radius varied from 0 cm (0 s) to ∼0.8 cm (2−8 s) and then stabilized at ∼1.1 cm (10−16 s). Accordingly, upon alternately applying and discharging the NIR stimulus, the surface paraffin of LR-PISS (tilt angle ≈ 9°) was transformed between liquid and solid states, and thereby the dynamic control between sliding and pinning for UGB (10 μL) could be readily achieved (Figure 1f and SI Movie S1). In water ambient, the generated heat at air−oil−solid platform (AOS) interface could not be absorbed because gas bubble prevents the heat flow into the surroundings due to its ultralow thermal-conductivity (SI Figure S7). For clarity, in a static water reservoir, the surface paraffin of LR-PISS would be melt for a slippery gaseous-bubble/liquid-paraffin/solid-PAF (GLS) system by virtue of NIR-triggered photothermal effect, which endows UGB with a smaller moving resistant force (f_{GLS}) and

https://dx.doi.org/10.1021/acsami.0c22717
ACS Appl. Mater. Interfaces 2021, 13, 9272−9280

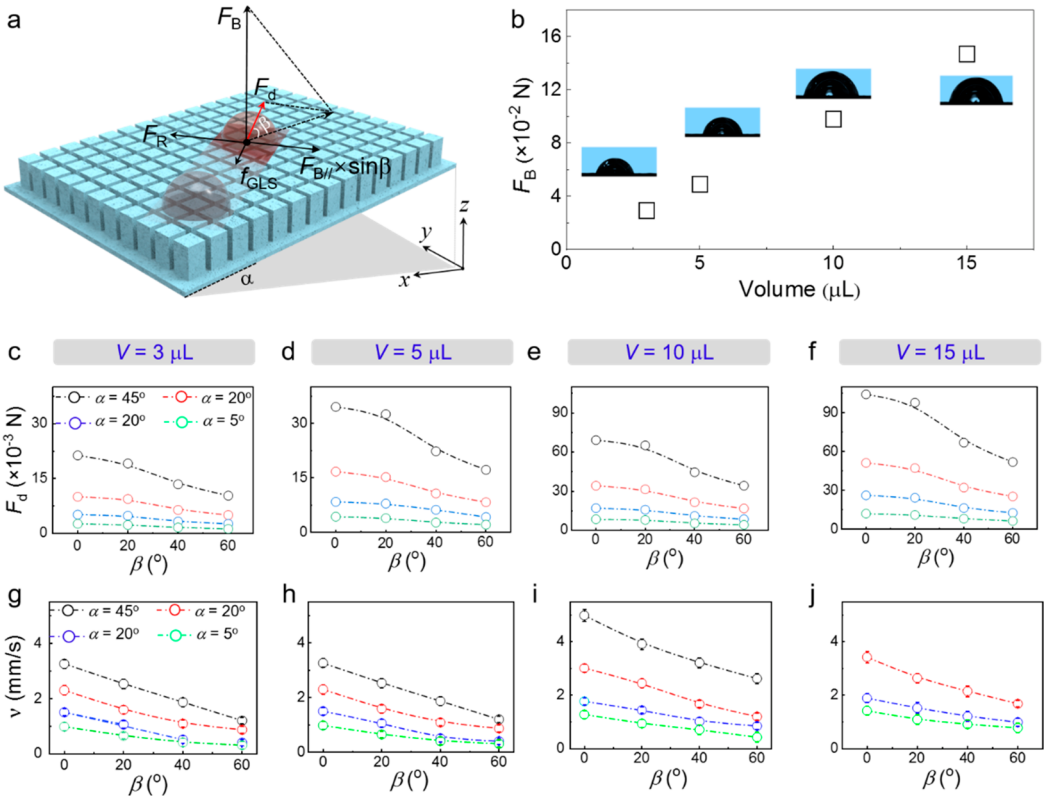

Figure 2. Newly explored steering hydrokinetics over various UGBs. (a) Physical model for NIR-actuating gasous bubble along a desirable route on LR-PISS. Therein, the moving behavior is dominated by a driven force derived buoyancy (F_d equal to $F_B$sin αcos β). (b) Buoyant force values for gasous bubbles with different volumes. (c–f) Numerical calculations for F_d in terms of different α, β, and V. (g–j) Evolution of recorded moving speed for multisized gasous bubbles under different α and β values.

contact angle hysteresis (F_{CAH}). Once the NIR-stimuli is removed, the UGB would immediately stick on smart LR-PISS depending on the reconfiguration of solid paraffin, which imparts UGB with a comparatively larger f_{GSS} and F_{CAH} (Figure 1f). Accordingly, the dynamic control over UGBs along either a slant or S-shaped pathways had been realized via on-demand harnessing the irradiating routes of NIR (Figure 1h,i; SI Figure S8 and SI Movies S2, S3, and S4). In comparison with previously reported SLIPS featuring with a single GLS system, current newly developed LR-PISS is more competent for facilely manipulating UGBs between sliding and pinning by the reversible evolution between the GLS system and GSS system, which is incapable of reaching this regulating strategy by virtue of other SLIPS. More importantly, current LR-PISS has unparalleled durability upon a solid lubricant in comparison with most reported SLIPS with liquid impregnations, which witness nonvolatile and environmental-benign merits, in addition to its temperature-triggered phase change feature.

2.2. Quantitative Study over Hydrokinetics of Steering Multisized UGBs Moving along Free Routes. In practical application, this newly developed SLIPS for manipulating UGBs with different size is highly desirable in terms of the water splitting,[11] gas-involved pressure sensor,[18] in addition to underwater ozone treatment.[19] In this part, we systematically studied the hydrodynamics over different bubbles steered by the NIR-stimuli. Typically, the force analysis for a UGB has been implemented for this free manipulation process (Figure 2a). Three crucial classical forces is considered to affect the steering of UGBs: (i) buoyant force (F_B) as a driving force is responsible for actuating UGB moving along NIR-irradiated path; (ii) a resistance, which is derived from the frictional force between the gasous bubble and liquid lubricant paraffin (f_{GLS}), is inverse to the moving direction; (iii) drag force (F_d) arising from three-phase (gesous bubble/liquid melt paraffin/solid unmelted paraffin) contact line, which provides a giant energy barrel for equilibrating the force of $F_B \times \sin \alpha \times \sin \beta$, is functional for preventing the UGB from derailing the moving parth. Therein, the domitant force for driving a UGB moving along free routes was defined as

$$F_{driven} = F_B \times \sin_\alpha \times \cos_\beta \quad (1)$$

where α is the tilt angle of the LR-PISS, β refers to the deviated angle of UGB from the axial direction on LR-PISS, and F_B representsthe buoyancy of UGB. Seen from this derivative equation, the larger the settled α, the larger the actuating force. In addition, the larger the bubble volume, the faster the sliding velocity because of a lager F_{driven}. In contrary, a larger β is unfavorable for accelerating the sliding of UGB along NIR-irradiated routes. Accordingly, for four typical UGBs with volumes of 3, 5, 10, and 15 μL, their F_B values is calculated as 2.9, 4.9, 9.8, and 14.7 ($\times 10^{-2}$) N (Figure 2b), respectively. As a result, their corresponding F_d values in terms of various α could be theoretically calculated according to above-derived equation (Figure 2c–f). Further, we carried out the experiments over the quantitative relationship amoung the sliding velocity (v) and bubble size (V) and α and β (Figure 2g–j), where we found that the moving velocity (v) tends to be slower with the increase of β and V, yet be comparatively faster

https://dx.doi.org/10.1021/acsami.0c22717
ACS Appl. Mater. Interfaces 2021, 13, 9272–9280

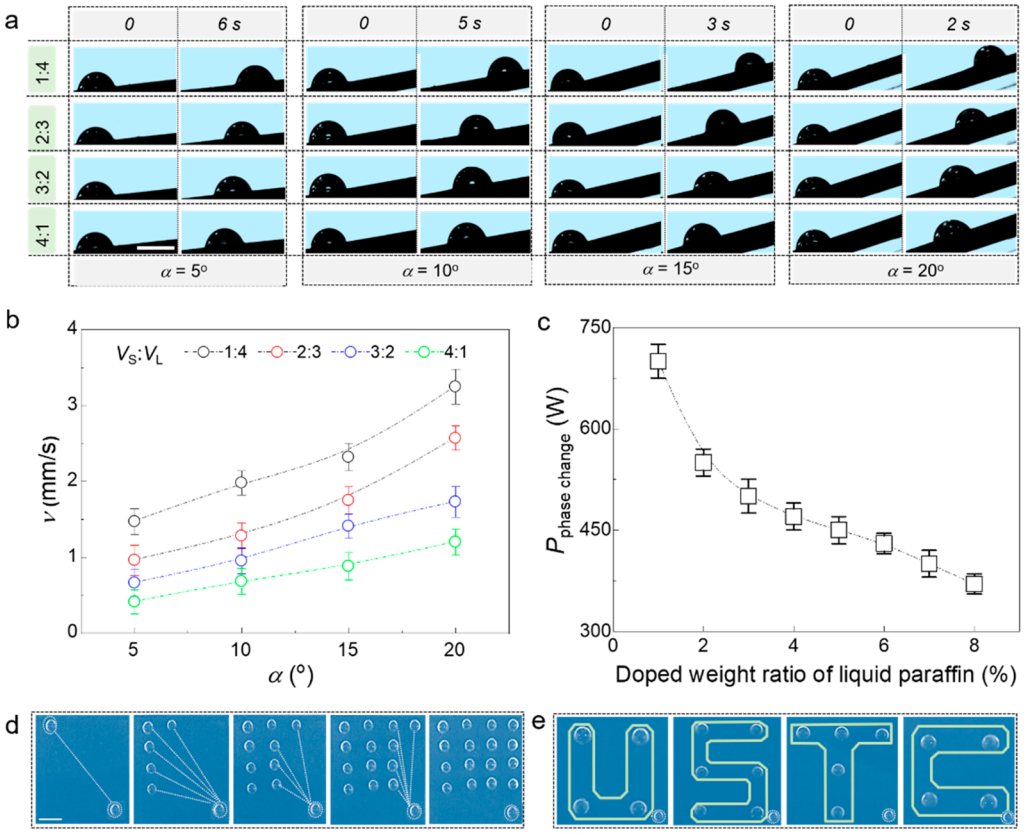

Figure 3. Effect of lubricant's recipe on steering performance. (a) Dynamic digital clips and (b) recorded sliding velocity for NIR-actuating UGBs (10 μL) on JR-PISSs under different α values that were impregnated with four doped ratios over a hybrid of solid paraffin wax and liquid paraffin oil. (c) Critical powers desired for melting the hybrid lubricant as a function of Fe_3O_4-doped content in JR-PISS, where the ratio of solid paraffin relative to liquid paraffin oil is ~2:3 (wt%). (d,e) Utilizing a optimized LR-PISS (tilt angle: ~10°) to steering gaseous bubbles for desirable patterns by remotely controlling the NIR-irradiating trace.

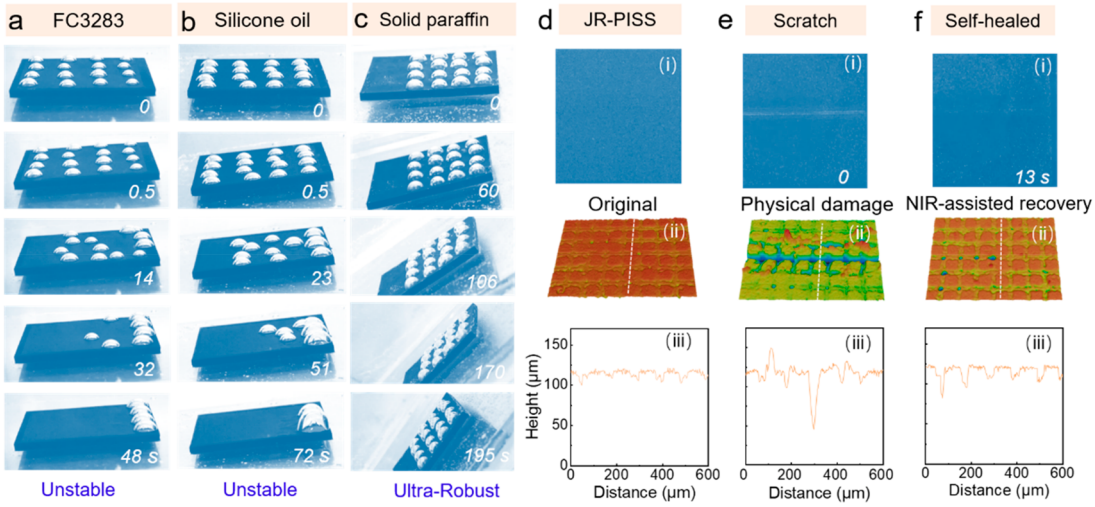

Figure 4. Ultrarobust LR-PISS with light-assisted self-healing ability. (a–c) Comparions of stability for UGBs arranged on FC-3283 (TA: ~3°), silicone oil (TA: ~3°), and current hybrid paraffin impregnated SLIPS (TA: ~10–65°), where the ambient is intentionally set as a flowing water. Digital pictures, 3D laser scanning profiles and line-scanning curves for displaying the (d) original, (e) physical-scratched, and (f) NIR-assisted self-healed LR-PISS. The results uncovers that current newly explored LR-PISS has unparallel stability and self-repairing capability in comparison with previously reported SLIPS.

with the elevation of α. The results is highly consistent with our constructed physic model as well as theoretical calculations. On the basis of fundamental physics, this part donates a kind of newly explored physical model in terms of steering UGBs along free routes, together with hydrokinetics over manipulating gaseous bubbles in liquid media, which is thus convinced to provide profound guidance for researchers occupied in microfluidics, bioinspired stimuli-responsive surfaces, and so on.

https://dx.doi.org/10.1021/acsami.0c22717
ACS Appl. Mater. Interfaces 2021, 13, 9272–9280

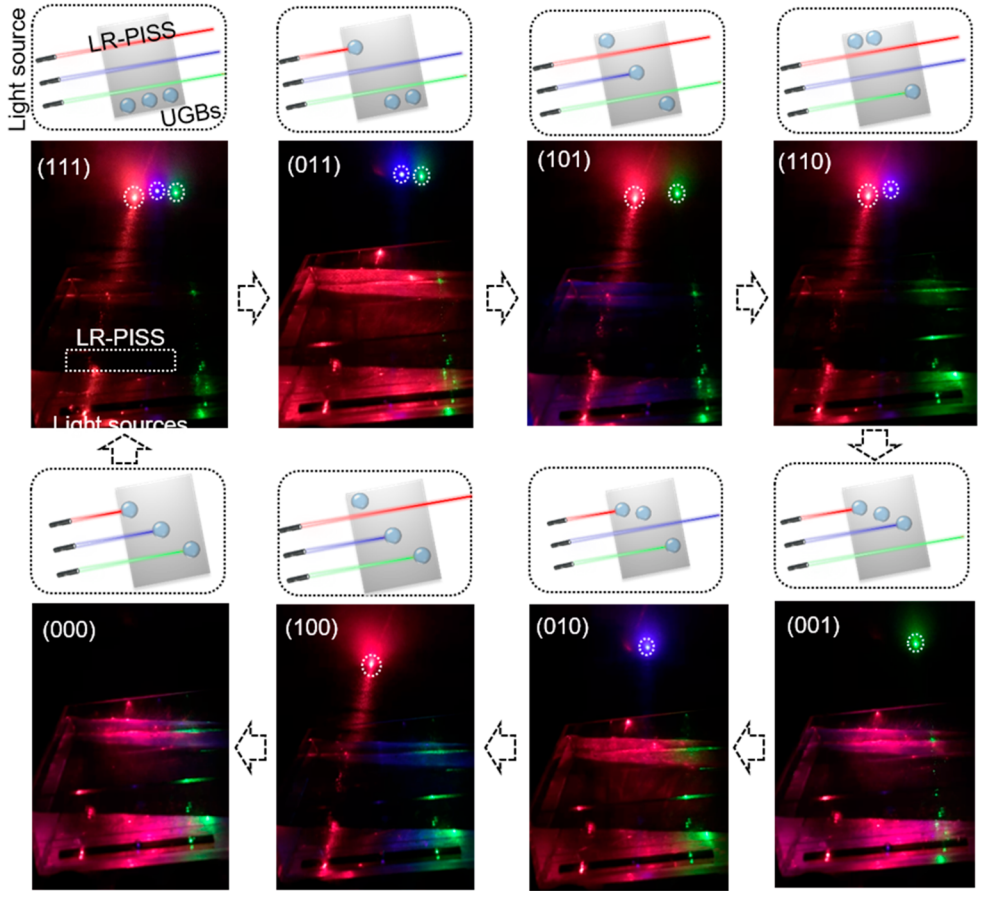

Figure 5. Free control of UGBs on LR-PISS for programmable light-path behaving as light-control-light optical shutter. Typically, serving as light shutters, UGBs could be actuated for programmable light-switch ranging from (111) to (000) on demand.

2.3. Effect of Lubricant'S Recipe on Steering Performance. Regardless of parameters including β (0°) and V (5 μL), we investigate the effect of lubricant's recipe (the doping ratio of solid paraffin wax and liquid paraffin oil) on the steering performance of gaseous bubble in liquid media. According to the previous explorations,[20,21] the liquid paraffin oil could be intentionally doped into the solid paraffin wax for decreasing the melting point of resultant lubricant, that is, a hybrid of solid/liquid mixed-phase. Herein, we selected a series of doping ratios including 1:4, 2:3, 3:2, and 4:1 serving as the hybrid lubricants that were infused into the as-prepared superhydrophic PDMS membranes, which was afterward employed for steering gasous bubbls at four α values of 5°, 10°, 15°, and 20°(Figure 3a), respectively. The results unfold that the moving velocity is prone to elevate with the increase of doping amount of liquid paraffin oil, which contributes to a smaller melting point for hybrid lubricants and thus donates a smaller interfacial frictional resistance as well as a smaller energy consumption arising from photothermal-effect (Figure 3b). Moreover, the critical power, which is defined as the minimum energy input required for inducing the hybrid lubricant' phase change ($P_{\text{phase-change}}$), is very limited to the doped ratio of Fe_3O_4 nanoparticals (NPs) behaving as the photothermal convertion media. Therefore, we study the relationship between $P_{\text{phase-change}}$ and doped weight ratio of Fe_3O_4−NPs, where we uncovered that the more the doped amount of Fe_3O_4−NPs, the smaller the input $P_{\text{phase-change}}$ (Figure 3c). Significantly, on the basis of above-explored steering hydrokinetics and quantitative investigations, programmable manipulation of gasous bubble is also harnessed by LR-PISS. Upon this light-triggered SLIPS, we unfold the capability of steering UGBs toward any targeted locations for their coalescence or constructing desired patterns (Figure 3d,e; SI Movie S5). Accordingly, people can select a desirable lubricant's recipe as well as an adaptive doped amount of Fe_3O_4−NPs for preparing light-responsive smart surfaces, which is then utilized for steering gasous bubbles in liquid media according to one's request.

2.4. Ultrarobust LR-PISS with Excellent Light-Assisted Self-Healing Ability. In comparison with previously explored rigid SLIPS, which is always lubricated with volatile silicone oil or FC3283 resulting in a limited longevity and feeble controlling ability, current LR-PISS is more responsible for steering UGBs through reversibly altering the lubricant's phase in resonse to NIR and unfolds ultrarobust sticking capability in terms of gaseous bubble (Figure 4a−c and SI Figure S9; SI Movie S6). More significantly, UGBs on paraffin-impregnated SLIPS can endure the enormous disturbance in flowing liquid environment at least 5 min, which manifest that current LR-PISS is adaptive for various liquid media even though a flowing one (SI Figure S10). Unfortunately, traditional FC3283/silicone oil-impregnated SLIPS tends to break down within several seconds. In practical usage, LR-PISS is inevitably subjected to abrasion or physical scratch, which would result in the invalidation of its steering performance. So, people always desire a kind of stimuli-responsive SLIPS having self-healing ability. Fortunately, seen from 3D laser profile images and line scanning curves, current LR-PISS is capable of in situ self-

https://dx.doi.org/10.1021/acsami.0c22717
ACS Appl. Mater. Interfaces 2021, 13, 9272−9280

healing in water under the assistance of remote NIR irradiation within 13 s, which should be favorable for the ultrafast performance reconfiguration over SLIPS and further enhancing the using longevity of the JR-PISS (Figure 4d–f and SI Figure S11; SI Movie S7). Once the LR-PISS suffers from physical damage, the severe loss of surface paraffin deteriorates the performance of SLIPS. Current light-responsive SLIPS could in situ self-repair in water ambient upon the capillary force among the micropillars, where the photothermal effect induced melting of unscratched paraffin wax would heal the wound for repairing the damaged SLIPS. As a candidate of emerging SLIPS, the ultrarobust JR-PISS with an ultrafast self-healing capability is convinced to harness dominant blockage in terms of utilizing longevity. Significantly, we have successfully actuated gaseous bubbles for application in light switch, where three light path could be switched ranging from all-switched-on (111) to all-switched-off (000) states by steering UGBs on LR-PISS for programmable opto-devices (Figure 5; SI Movie S8).

3. CONCLUSION

In summary, we have put forward a light-responsive slippery surface composed of superhydrohobic micropillar-arraryed Fe_3O_4/PDMS platform fabricated by one-step femtosecond laser ablation and lubricant paraffin wax. Upon this newly explored smart SLIPS, the dynamic motion control over UGBs could be reversibley swiched between pining and sliding by loading/discharging remote NIR-stimuli. The underlying mechanism is that when the NIR was applied, the UGBs would be actuated to slide along the NIR-irradiated trace, which was melt for a slippery surface having a smaller F_{CAH} within 1.0 s. Once the NIR was removed, the liquefied paraffin would be reconfigured to solid phase for pinning a moving UGB within 0.5 s due to the revovered frictional nonslippery one with larger F_{CAH}. On the basis of newly explored hydrokinetics, we quantitatively study the effect of bubble volume (V), inclined angles (α /β), and lubricant recipe on the moving velocity (ν) of UGBs. Fundamental basis rendered us steering gaseous bubbles toward any desirable patterns and exihibiting great potential in light-control-light optical shutter. More importantly, compared with previously reported slippery surfaces, current LR-PISS is more competent for imparting UGBs with ultrarobust antidisturbance capability even in flowing liquid environment. Further, even subjected to physical damage, current light-triggered SLIPS is able to self-heal in situ within 13 s under the assistance of remote NIR. The results suggest a manipulating principle for robust bioinspired bubble actuator.

4. EXPERIMENTAL SECTION

4.1. Materials. Fe_3O_4NPs (diameter: 10 nm, purity: 99.9%) was purchased from Kelly Institute of Metallurgy (Tianjin, China). PDMS (Sylgard 184 Kits) elastomer was purchased from the Dow Corning (Auburn, MI). Paraffin wax was provided by Sigma-Aldrich. Liquid paraffin oil was donated by Guangzhou Changrong Chemical Co. Ltd., FC3283 were provided by Shengzheng Sino-Fluorine Technology Co., Ltd. Silicone oil (100 mPa·s) was purchased from Dow Corning. Distilled water (H_2O, density: 1 g·cm^{-3}) were used as contact angle test materials. NIR Light Source: The NIR light with wavelength of 808 nm (power: 800 mw, spot sera: 5.6 × 4.5 mm$^{2)}$ was purchased from Fuzhe Technology Co., Ltd., China, BY adjusting with the support bracket. The irradiation distance of NIR could be adjusted in the range of 20–80 cm, the irradiation distance of NIR was set as 20 cm in this work.

4.2. Bulding of LR-PISS. First, the PDMS base polymer and curing agent (mass ratio: 10:1) are mixed together, and mechanically stirred at 1000 rpm for 20 min. Then, the Fe_3O_4 nanoparticles are added to PDMS by manual stirring. The mixture was mixed at 1500 rpm for 10 min, and then the homogeneous mixture was poured into the cube grinding tool, and vacuum treatment was performed for 30 min to remove air bubbles in the liquid. Then it was cured at 100 °C for 3 h. Finally, the cured Fe_3O_4–NPs/PDMS composite was peeled off the mold. Micropillar arrays with three-level micro/nano structures can be manufactured in cross-scan mode with femtosecond lasers. A laser beam (104 fs, 1 kHz, 800 nm) from a regeneratively amplified Ti: Sapphire femtosecond laser system (Legend Elite-1K-HE, Coherent, Santa Clara, CA) was used for ablation, and the femtosecond laser power, scanning spacing and speed were set at 200 mW, 150 μm, and 4 mm·s^{-1}, respectively. Putting the PFA on the heating plate and place the mixed paraffin from being on the surface. With the help of heat, the paraffin will be melted and diffused for 1 h, and then it will be buckled upside down on a glass shelf to remove the excess paraffin, and finally placed at room temperature for annealing and solidification.

4.3. Characterization. The micronanostructure induced by the femtosecond laser were observed by using a field-emission scanning electron microscope (JSM-7500F, Japan) at 5 kV. The contact angles of the water droplet (5 μL) in the air were characterized by a CA100C contact-angle system (Innuo, China) with the sessile drop method, The measured value was derived from the average of five measurements at different locations on the same film. The contact angle measurement environment was 20 °C and 10% humidity. The infrared thermal images of irradiated LR-PASS under NIR were observed by an thermal infrared camera (VarioCAMhr head 680, InfraTec) at 25 °C temperature. The videos for displaying the current light-responsive bubble manipulation were record by the mobile phone(iphone-6 plus) at a resolution of 1920 × 1080 and 30 fps.

■ ASSOCIATED CONTENT

Supporting Information

The Supporting Information is available free of charge at https://pubs.acs.org/doi/10.1021/acsami.0c22717.

XRD spectra for PDMS membrane, Fe_3O_4 nanoparticles, pristine Fe_3O_4-doped PDMS and laser-ablated PAF, high-resolution SEM images for fs laser induced nanoporous and nanoparticles on PAF, digital pictures for unfolding the weight variation and 3D profile and line scanning curves for PAF and LR-PISS, schematic diagram for unfolding the NIR-irradiated LR-PISS in air and water surroundings, the NIR-irradiated LR-PISS in water surrounding, the thermo-dynamics over NIR-irradiated UGBs, FTIR images for NIR-tracing free routes on LR-PISS, longevity test of LR-PISS suffering from bubble sliding for multiple-times, comparisons of stability for UGBs arranged on three different lubricant indused surfaces, LR-PISS with light-assisted self-healing precess (PDF)

Light-driven smart control over UGBs between pinning and sliding (MP4)

Light-driven UGB sliding along slant route (MP4)

Light-driven UGB moving along S-shaped route (MP4)

NIR-tracing free routes on LR-PISS (MP4)

Light-driven UGBs toward desirable pattern (MP4)

Antidisturbance performance comparison for three typical SLIPS (MP4)

Light-assisted in situ self-healing in water environment (MP4)

Light-driven UGBs on LR-PISS for programmable ligh-control-light optical shutter (MP4)

https://dx.doi.org/10.1021/acsami.0c22717
ACS Appl. Mater. Interfaces 2021, 13, 9272–9280

AUTHOR INFORMATION

Corresponding Authors

Jiawen Li − *CAS Key Laboratory of Mechanical Behavior and Design of Materials, Key Laboratory of Precision Scientific Instrumentation of Anhui Higher Education Institutes. Department of Precision Machinery and Precision Instrumentation, University of Science and Technology of China, Hefei 230026, China*; Email: jwl@ustc.edu.cn

Dong Wu − *CAS Key Laboratory of Mechanical Behavior and Design of Materials, Key Laboratory of Precision Scientific Instrumentation of Anhui Higher Education Institutes. Department of Precision Machinery and Precision Instrumentation, University of Science and Technology of China, Hefei 230026, China*; orcid.org/0000-0003-0623-1515; Email: dongwu@ustc.edu.cn

Authors

Zhouchen Huang − *CAS Key Laboratory of Mechanical Behavior and Design of Materials, Key Laboratory of Precision Scientific Instrumentation of Anhui Higher Education Institutes. Department of Precision Machinery and Precision Instrumentation, University of Science and Technology of China, Hefei 230026, China*

Chao Chen − *CAS Key Laboratory of Mechanical Behavior and Design of Materials, Key Laboratory of Precision Scientific Instrumentation of Anhui Higher Education Institutes. Department of Precision Machinery and Precision Instrumentation, University of Science and Technology of China, Hefei 230026, China*

Xinghao Wang − *CAS Key Laboratory of Mechanical Behavior and Design of Materials, Key Laboratory of Precision Scientific Instrumentation of Anhui Higher Education Institutes. Department of Precision Machinery and Precision Instrumentation, University of Science and Technology of China, Hefei 230026, China*

Rui Li − *CAS Key Laboratory of Mechanical Behavior and Design of Materials, Key Laboratory of Precision Scientific Instrumentation of Anhui Higher Education Institutes. Department of Precision Machinery and Precision Instrumentation, University of Science and Technology of China, Hefei 230026, China*

Yucheng Bian − *CAS Key Laboratory of Mechanical Behavior and Design of Materials, Key Laboratory of Precision Scientific Instrumentation of Anhui Higher Education Institutes. Department of Precision Machinery and Precision Instrumentation, University of Science and Technology of China, Hefei 230026, China*

Suwan Zhu − *CAS Key Laboratory of Mechanical Behavior and Design of Materials, Key Laboratory of Precision Scientific Instrumentation of Anhui Higher Education Institutes. Department of Precision Machinery and Precision Instrumentation, University of Science and Technology of China, Hefei 230026, China*; orcid.org/0000-0001-9881-5694

Yanlei Hu − *CAS Key Laboratory of Mechanical Behavior and Design of Materials, Key Laboratory of Precision Scientific Instrumentation of Anhui Higher Education Institutes. Department of Precision Machinery and Precision Instrumentation, University of Science and Technology of China, Hefei 230026, China*; orcid.org/0000-0003-1964-0043

Jiaru Chu − *CAS Key Laboratory of Mechanical Behavior and Design of Materials, Key Laboratory of Precision Scientific Instrumentation of Anhui Higher Education Institutes. Department of Precision Machinery and Precision Instrumentation, University of Science and Technology of China, Hefei 230026, China*; orcid.org/0000-0001-6472-8103

Complete contact information is available at: https://pubs.acs.org/10.1021/acsami.0c22717

Author Contributions

[a]Z.H. and C.C. contributed equally to this work

Notes

The authors declare no competing financial interest.

ACKNOWLEDGMENTS

This work was supported by the National Natural Science Foundation of China (Nos. 52005475, 51875544, 61805230), National Key Scientific Instrument and Equipment Development Project (No. 61927814), Fundamental Research Funds for the Central Universities (WK2090090024, WK6030000113) and the National Key R&D Program of China (2017YFB1104303, 2018YFB1105400).

REFERENCES

(1) Anna, S. L. Droplets and Bubbles in Microfluidic Devices. *Annu. Rev. Fluid Mech.* **2016**, *48*, 285−309.

(2) Ødegaard, H. The Use of Dissolved Air Flotation in Municipal Wastewater Treatment. *Water Sci. Technol.* **2001**, *43*, 75−81.

(3) Lu, Z.; Zhu, W.; Yu, X.; Zhang, H.; Li, Y.; Sun, X.; Wang, X.; Wang, H.; Wang, J.; Luo, J.; Lei, X.; Jiang, L. Ultrahigh Hydrogen Evolution Performance of Under-Water "Superaerophobic" MoS_2 Nanostructured Electrodes. *Adv. Mater.* **2014**, *26*, 2683−2687.

(4) Li, Y.; Zhang, H.; Xu, T.; Lu, Z.; Wu, X.; Wan, P.; Sun, X.; Jiang, L. Under-Water Superaerophobic Pine-Shaped Pt Nanoarray Electrode for Ultrahigh-Performance Hydrogen Evolution. *Adv. Funct. Mater.* **2015**, *25*, 1737−1744.

(5) Reynolds, C.; Yitayew, M. Low-Head Bubbler Irrigation Systems. Part II. Air Lock Problems. *Agric. Water Manage.* **1995**, *29*, 25−35.

(6) Philipp, A.; Lauterborn, W. Cavitation Erosion by Single Laser-Produced Bubbles. *J. Fluid Mech.* **1998**, *361*, 75−116.

(7) Fairfield, C. Cavitation Damage to Potential Sewer and Drain Pipe Materials. *Wear* **2014**, *317*, 92−103.

(8) Fontanesi, S.; Giacopini, M.; Cicalese, G.; Sissa, S.; Fantoni, S. Numerical Investigation of the Cavitation Damage in the Wet Cylinder Liner of a High Performance Motorbike Engine. *Eng. Failure Anal.* **2014**, *44*, 408−423.

(9) Yu, C.; Cao, M.; Dong, Z.; Wang, J.; Li, K.; Jiang, L. Spontaneous and Directional Transportation of Gas Bubbes on Superhydrophobic Cones. *Adv. Funct. Mater.* **2016**, *19*, 3236−3243.

(10) Zhu, S.; Bian, Y.; Wu, T.; Li, E.; Li, J.; Hu, Y.; Wu, D.; Chu, J. Spontaneous and Unidirectional Transportation of Underwater Bubbles on Superhydrophobic Dual rails. *Appl. Phys. Lett.* **2020**, *116*, 093706.

(11) Long, Z.; Zhao, Y.; Zhang, C.; Zhang, Y.; Yu, C.; Wu, Y.; Ma, J.; Cao, M.; Jiang, L. A Multi-Bioinspired Dual-Gradient Electrode for Microbubble Manipulation toward Controllable Water Splitting. *Adv. Mater.* **2020**, *32*, 1908099.

(12) Zhang, J.; Liu, P.; Yi, B.; Wang, Z.; Huang, X.; Jiang, L.; Yao, X. Bio-Inspired Elastic Liquid-Infused Material for On-Demand Underwater Manipulation of Air Bubbles. *ACS Nano* **2019**, *13*, 10596−10602.

(13) Wong, T. S.; Kang, S. H.; Tang, S. K.; Smythe, E. J.; Hatton, B. D.; Grinthal, A.; Aizenberg, J. Bioinspired Self-Repairing Slippery Surfaces with Pressure-Stable Omniphobicity. *Nature* **2011**, *477*, 443−447.

(14) Yu, C.; Zhu, X.; Li, K.; Cao, M.; Jiang, L. Manipulating Bubbles in Aqueous Environment via a Lubricant-Infused Slippery Surface. *Adv. Funct. Mater.* **2017**, *27*, 1701605.
(15) Guo, P.; Wang, Z.; Heng, L.; Zhang, Y.; Wang, X.; Jiang, L. Magnetocontrollable Droplet and Bubble Manipulation on a Stable Amphibious Slippery Gel Surface. *Adv. Funct. Mater.* **2019**, *29*, 1808717.
(16) Chen, C.; Huang, Z.; Shi, L. A.; Jiao, Y.; Zhu, S.; Li, J.; Hu, Y.; Chu, J.; Wu, D.; Jiang, L. Remote Photothermal Actuation of Underwater Bubble toward Arbitrary Direction on Planar Slippery Fe3O4-Doped Surfaces. *Adv. Funct. Mater.* **2019**, *29*, 1904766.
(17) Zhu, S.; Bian, Y.; Wu, T.; Chen, C.; Jiao, Y.; Jiang, Z.; Huang, Z.; Li, E.; Li, J.; Chu, J.; Hu, Y.; Wu, D.; Jiang, L. High Performance Bubble Manipulation on Ferrofluid-Infused Laser-Ablated Microstructured Surfaces. *Nano Lett.* **2020**, *20*, 5513−5521.
(18) Xue, X.; Wang, R.; Lan, L.; Wang, J.; Xue, Z.; Jiang, L. Reliable Manipulation of Gas Bubble Size on Superaerophilic Cones in Aqueous Media. *ACS Appl. Mater. Interfaces* **2018**, *10*, 5099−5106.
(19) Xia, Z.; Hu, L. Treatment of Organics Contaminated Wastewater by Ozone Micro-Nano-Bubbles. *Water* **2019**, *11*, 55.
(20) Manabe, K.; Matsubayashi, T.; Tenjimbayashi, M.; Moriya, T.; Tsuge, Y.; Kyung, K.-H.; Shiratori, S. Controllable Broadband Optical Transparency and Wettability Switching of Temperature-Activated Solid/Liquid-Infused Nanofibrous Membranes. *ACS Nano* **2016**, *10*, 9387−9396.
(21) Chen, C.; Zhou, L.; Shi, L. A.; Zhu, S.; Huang, Z.; Xue, C.; Li, J.; Hu, Y.; Wu, D.; Chu, J. Ultralow-Voltage-Driven Smart Control of Diverse Drop's Anisotropic Sliding by in Situ Switching Joule Heat on Paraffin-Infused Microgrooved Slippery Surface. *ACS Appl. Mater. Interfaces* **2020**, *12*, 1895−1904.
(22) Jiao, Y.; Lv, X.; Zhang, Y.; Li, C.; Li, J.; Wu, H.; Xiao, Y.; Wu, S.; Hu, Y.; Wu, D.; Chu, J. Pitcher Plant-Bioinspired Bubble Slippery Surface Fabricated by Femtosecond Laser for Buoyancy-Driven Bubble Self-Transport and Efficient Gas Capture. *Nanoscale* **2019**, *11*, 1370−1378.
(23) Lv, X.; Jiao, Y.; Wu, S.; Li, C.; Zhang, Y.; Li, J.; Hu, Y.; Wu, D. Anisotropic Sliding of Underwater Bubbles on Microgrooved Slippery Surfaces by One-Step Femtosecond Laser Scanning. *ACS Appl. Mater. Interfaces* **2019**, *11*, 20574−20580.
(24) Djogo, G.; Li, J.; Ho, S.; Haque, M.; Ertorer, E.; Liu, J.; Song, X.; Song, J.; Herman, P. R. Femtosecond Laser Additive and Subtractive Micro-Processing: Enabling a High-Channel-Density Silica Interposer for Multicore Fibre to Silicon-Photonic Packaging. *Int. J. Extrem. Manuf.* **2019**, *1*, 045002.
(25) Zhang, Y.; Jiao, Y.; Li, C.; Chen, C.; Li, J.; Hu, Y.; Wu, D.; Chu, J. Bioinspired Micro/Nanostructured Surfaces Prepared by Femtosecond Laser Direct Writing for Multi-Functional Applications. *Int. J. Extrem. Manuf.* **2020**, *2*, 032002.
(26) Bai, X.; Yang, Q.; Fang, Y.; Zhang, J.; Yong, J.; Hou, X.; Chen, F. Superhydrophobicity-Memory Surfaces Prepared by a Femtosecond Laser. *Chem. Eng. J.* **2020**, *383*, 123143.
(27) Zhang, J.; Zhang, K.; Yong, J.; Yang, Q.; He, Y.; Zhang, C.; Hou, X.; Chen, F. Femtosecond Laser Preparing Patternable Liquid-Metal-Repellent Surface for Flexible Electronics. *J. Colloid Interface Sci.* **2020**, *578*, 146−154.
(28) Xiong, W.; Zhou, Y.; Hou, W.; Jiang, L.; Mahjouri-Samani, M.; Park, J.; He, X.; Gao, Y.; Fan, L.; Baldacchini, T.; Silvain, J.; Lu, Y. Laser-Based Micro/Nanofabrication in One, Two and Three Dimensions. *Front. Optoelectron.* **2015**, *8*, 351−378.

https://dx.doi.org/10.1021/acsami.0c22717
ACS Appl. Mater. Interfaces 2021, 13, 9272−9280